Bull. Astr. Soc. India (1997) **25**, 253–279

Nonlinear propagation of intense electromagnetic waves in quasar and pulsar plasmas

R.T. Gangadhara*

Indian Institute of Astrophysics, Bangalore 560 034, India

Abstract. We present the results of analytical as well as numerical investigations of radiation–plasma interaction instabilities in astrophysical plasmas. We consider the stimulated Raman and Compton scattering in the continuum emission of quasars. There are three ways in which an electromagnetic wave can undergo scattering in a plasma : (i) when the scattering of radiation occurs by a single electron, it is called Compton scattering; (ii) if it occurs by a longitudinal electron plasma mode, it is called Stimulated Raman Scattering (SRS), and (iii) if it occurs by a highly damped electron plasma mode, it is called Stimulated Compton Scattering. The non-thermal continuum of quasars is believed to be produced through the combined action of synchrotron and inverse Compton processes, which are essentialy single particle processes. We have shown as an example that the complete spectrum of 3C 273 can be reproduced by suitably combining Stimulated Compton Scattering and SRS (Gangadhara and Krishan 1992). The differential contributions of these stimulated scattering processes under different values of the plasma parameters are also calculated.

The coherent plasma process such as parametric decay instability in a homogeneous and unmagnetized plasma, cause anomalous absorption of intense electromagnetic radiation under specific conditions of energy and momentum conservation and thus cause anomalous heating of the plasma. The maximum plasma temperatures reached are functions of luminosity of the radio radiation and plasma parameters. It is believed that these processes may be taking place in many astrophysical objects. These processes can also contribute towards the absorption of 21-cm radiation, which is otherwise mostly attributed to neutral hydrogen regions (Krishan 1988).

The change in polarization of an electromagnetic wave can occur due to SRS in a plasma. In this process an electromagnetic wave undergoes coherent scattering off an electron plasma wave. It is found that some of the observed polarization properties such as the rapid temporal variations, sense reversal, rotation of the plane of polarization and change of nature of polarization in the case of pulsars and quasars, could be accounted for through SRS.

* Present address : Max Planck-Institute für Radio-astronomie, Auf dem Hügel 69, 53121 Bonn, Germany.

The modulational instability of a large-amplitude electromagnetic wave in an electron-positron plasma, can excite due to the effect of relativistic mass variation of the plasma particles, harmonic generation, and the non-resonant, finite frequency electrostatic density perturbations, all caused by the large-amplitude radiation field. The radiation from many strong sources such as quasars and pulsars, has been observed to vary over a host of time-scales. It is possible that extremely rapid variations in the non-thermal continuum of quasars as well as in the non-thermal radio radiation from pulsars can be accounted for by the modulational instabilities to which the radiation may be subjected during its propagation out of the emission region.

1. Introduction

It is generally believed that the Universe is a plasma. A plasma, by nature is hyperactive. More often than not, it responds violently to external stimuli in an attempt to attain equilibrium. An important feature of the electromagnetic wave propagation in an istotropic and unmagnetized plasma, is a cutoff (dielectric function ϵ vanishes) at the plasma frequency; an electromagnetic wave with frequency less than the plasma frequency cannot propagate in the plasma. Since plasma frequency is proportional to the square root of the charged particles density, the density fluctuations in interstellar space create local variations in the velocity and direction of propagation of radio waves. The frequency of the electromagnetic wave for which its phase velocity vanishes, is called as resonance frequency. The electromagnetic waves at resonance are strongly absorbed in a plasma.

When a plasma is subjected to the electric field of an high-intensity electromagnetic wave, it exhibits a variety of non-linear processes which modify the plasma parameters as well as those of the electromagnetic waves. When the size of the plasma region disturbed by the electromagnetic wave is much larger than the mean free path of an electron, the electron can gain enough energy before suffering collisions with other ions and neutrals. Further the large mass difference between electron and other particles hinder the transfer of energy from electrons to the heavy particles. Thus the electric field of the electromagnetic wave heats the electrons preferentially, as a result of which the dielectric function ϵ and the conductivity σ of the plasma become functions of the electromagnetic wave field and a non-linear relation between the electric field $\vec{E}$ and the current density $\vec{J} = \sigma(\vec{E})\,\vec{E}$ is set up. In the opposite case, when the size of the disturbed plasma region is much smaller than the mean free path of an electron, the inhomogeneous electric field of the electromagnetic wave exerts a pressure on the electrons, creating compressions and rarefactions. Thus, the dielectric function begins to depend on the electromagnetic wave field and the plasma again becomes a non-linear medium. Summarizing, a collisional plasma becomes a non-linear mainly through the dependence of electron temperature on the electromagnetic wave field and a collisionless plasma becomes non-linear mainly through the dependence of electron density on the electromagnetic wave field. In such a non-linear medium, electromagnetic wave undergoes anonmalous absorption, anomalous scattering, modulation and polarization change. In this thesis, the role of these non-linear plasma processes in the functioning of quasars and pulsars is investigated.

1.1 Quasars

Quasars and active galactic nuclei (AGN) are the most luminous objects in the universe. It is generally believed that they consist of a central engine, perhaps a supermassive ($M = 10^8 - 10^9$ $M_\odot$) black hole powered by the accreting matter. Fig. 1 shows a schematic representation of a quasar with Schwarzschild radius $R_s = 2GM / c^2 = 2.95 \times 10^{13}$ M_8 cm, where $M = M_8 \times 10^8$ $M_\odot$. The power-law spectrum and high brightness temperature ~ 10^{19} K clearly indicate the nonthermal radiation mechanisms occuring in quasars and AGN. We expect the plasma processes to play an important role in the emission from the broad as well as narrow line regions.

Collective plasma processes play a major role in the energy dissipation of jets at the hot spots of extragalactic radio sources (Lesch *et al.* 1989). The polarization measurements by Röser and Meisenheimer (1987) have proved beyond doubt that the hot spot emission is non-thermal. It is generally agreed that jets provide links between the central activity and the hot spots.

In strong radio sources, the rapid temporal variations, sense reversal, rotation of plane of polarization and change of nature of polarization can be accounted for through SRS.

Observations have revealed that many compact radio sources, in addition to the usual long-term variability, possess an intrinsic variability with time-scales less than a day. Heeschen *et al.* (1987) found, quite unexpectedly, the variations of ~ 1 day at a wavelength of 11 cm in several flat-spectrum sources. Observations of intraday radio variability in compact radio sources and their probable explanations are given by Quirrenbach (1990).

We believe a plasma process such as the modulational instablity may be a potential mechanism for rapid variability in quasars and BL Lacs. Low frequency electrostatic density perturbations are non-linearly excited due to the interaction of a large amplitude electromagnetic wave with a plasma. The superposition of low-frequency oscillation (electrostatic wave) over an high-frequency wave (electromagnetic wave) produce an amplitude-modulated electromagnetic wave (Gangadhara *et al.* 1993).

1.2 Pulsars

The radio emission is believed to occur from each magnetic pole of a pulsar, with an angular width of the order of 10°. The magnetic axis and the line of sight may be arbitrarily oriented with respect to the rotation axis of the pulsar. The geometry of the pulsar polar cap emission is shown in the Fig. 2. The observer sees radiation from the point P, which moves across the arc ST as the pulsar rotates. The zero of the longitude ϕ starts at the meridian through the rotation axis, and position angle ψ is measured with respect to the projected direction of the magnetic axis.

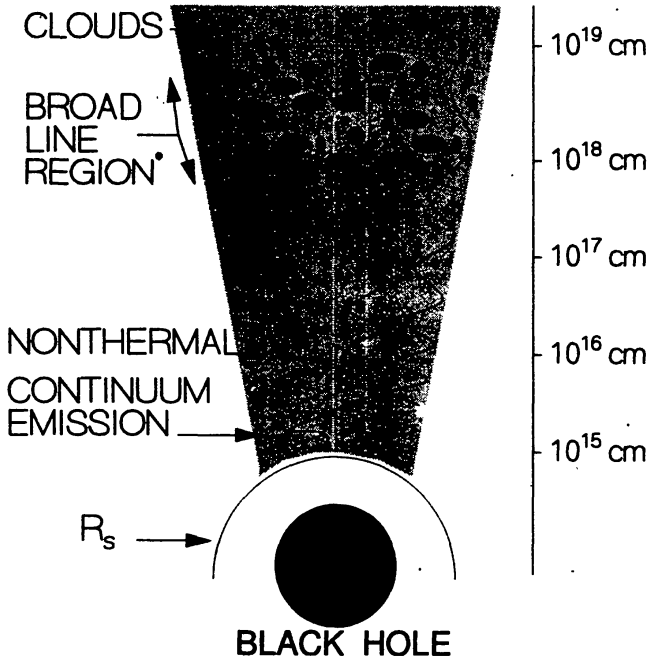

Figure 1. Schematic representation of a quasar.

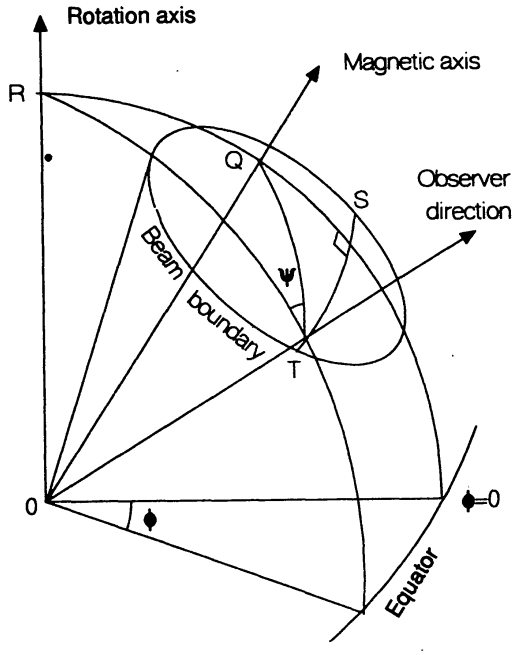

Figure 2. The geometry of pulsar beams.

The radio pulse occurs during a small fraction of the period, corresponding to between 5° and 20° of angular rotation, for most pulsars. Due to the rotation of the pulsar, the beam of radiation sweeps across the line of sight of the observer and it forms a pulse at each rotation, in analogy with the lighthouse. The high energy plasma particles moving along the curved magnetic field lines emit a beam of radiation. Because of magnetic field, the source of radiation is rigidly attached to the solid surface of the neutron star. The emission occurs at a radial distance of about a few tens of neutron star radius (~ 10 km). High freqency radiation is emitted at lower radius while frequency radiation at higher radius of the beam.

The intensities of the pulsar radio emission are extremely high and are observed to fluctuate on several time scales. Therefore, the radio radiation cannot be due to thermal emission or incoherent syncrotron emission. It is therefore concluded that the sources of radio emission are **coherent**. Coherent emission is also implied by the high-intensity of the radio sources. For the Crab pulsar the brightness temperature estimated for the radio spectrum exceeds 10^{30} K. Pulsars have power-law spectra $F \sim \nu^{-\alpha}$ at radio frequencies. The spectral index α lies between about 1 and 3, with a low energy cutoff and the flux density F is normally of the order of 1 Jansky.

The individual radio pulses are often observed to be hightly variable in intensity as well as in polarization. However, the integrated pulse profile obtained by the superimposition of some $10^3 - 10^4$ recorded pulses is stable and a unique characteristic of each pulsar.

The anomalous absorption of radio waves can take place in pulsars also, and the rate of anomalous absorption of radio radiation in Crab Nebula is much higher than that due to collisional absorption rate (Gangadhara and Krishan 1990).

Many pulsars have subpulses or quasi-periodic sequences of subpulses, called as 'periodic microstructures'. Measurements with time resolutions ≤ 1 msec show subpulse structure with characteristic widths of several percent of the period. But for resolutions ≤ 1 μsec the subpulses of some pulsars exhibit microstructure with widths of the order of $\sim 10^{-3}$ P, where P is the period of a pulsar. This fine structure is usually regarded as **modulation** of the radiation by the noise (Cordes 1983; Lyne & Graham–Smith 1990; Gangadhara *et al.* 1993).

The radio emission from many pulsars shows linear and often circular or elliptical polarization. The integrated pulse profile may have a high-average polarization and the position angle of the linearly polarized component swings monotonically through the integrated pulse by an angle up to 180°. In some cases (e.g., Vela, PSR 0833–45) essentially all the integrated profile is linearly polarized while in others circular component is seen near the center of the pulse. The sense of circular polarization may remain same throughout the pulse or it may reverse (Manchester and Taylor 1977). Roughly, about 20 percent of the profile is circularly polarized. The change of polarization properties, such as sense reversal, rotation of the polarization plane and degree, on extremely short time scales can occur due to the SRS (Gangadhara and Krishan, 1993, 1995). In the next section we consider a very important case of parametric instability, the change of polarization due to SRS.

2. Polarization changes of radiation through SRS

We begin with a model consisting of a pulsar with non-thermal component of radiation interacting with the plasma in the emission region at a distance $r = 100\ R_{NS} = 10^8$ cm (Neutron star radius $R_{NS} \approx 10$ km). In the case of a quasar, we consider a black hole surrounded by a plasma which extends to a few parsecs. The non-thermal continuum is considered as a pump which drives SRS. Here, we consider an electoron-ion plasma with uniform and isotropic distribution of temperature and density, and assume that it is at rest with respect to the source of radiation.

Consider a large amplitude elliptically polarized electromagnetic wave,

$$\vec{E_i} = \epsilon_i [\cos (\vec{k_i} . \vec{r} - \omega_i t)\, \hat{e}_1 + \alpha_i \cos (\vec{k_i} . \vec{r} - \omega_i t + \delta i)\, \hat{e}_2], \tag{1}$$

propagating in a plasma with density n_0 and temperature T_e.

We can think of $\vec{E_i}$ as the superposition of two linearly polarized waves

$\vec{E_{i1}} = \epsilon_i \cos (\vec{k_i} . \vec{r} - \omega_i t)\, \hat{e}_1$ and $\vec{E_{i2}} = \alpha_i \epsilon_i \cos (\vec{k_i} . \vec{r} - \omega_i t + \delta_i)\, \hat{e}_2$.

Let $\delta n_{e1} = \delta n_1 \cos (\vec{k} . \vec{r} - \omega t)$ (2)

and

$$\delta n_{e2} = \delta n_2 \cos (\vec{k} . \vec{r} - \omega t + \delta_e), \tag{3}$$

be the density perturbations in a plasma with equilibrium density n_0. Assume that δn_{e1} couples with $\vec{E_{i1}}$ and δn_{e2} couples with $\vec{E_{i2}}$. The coupling between the radiation and the density perturbations is non-linear because of the ponderomotive force ($\propto \nabla E_{i1}^2$ and $\propto \nabla E_{i2}^2$). Consequently, density perturbations grow up and lead to currents at $(\vec{k_i} \pm \vec{k}, \omega_i \pm \omega)$. These currents will generate mixed electromagnetic-electrostatic side-band modes at $(\vec{k_i} \pm \vec{k}, \omega_i \pm \omega)$. The side-band modes, in turn, interact with the incident wave field, producing a ponderomotive force which amplifies the original density perturbation. Thus, there is a positive feedback system which leads to an instablity.

The electric field $\vec{E_s}$ of the electromagnetic wave scattered through an angle ϕ_s with respect to $\vec{k_i}$ can be witten as

$$\vec{E_s} = \epsilon_s [\cos (\vec{E_s} . \vec{r} - \omega_s t)\, \hat{e}_1' + \alpha_s \cos (\vec{k_s} . \vec{r} - \omega_s t + \delta_s)\, \hat{e}_2']. \tag{4}$$

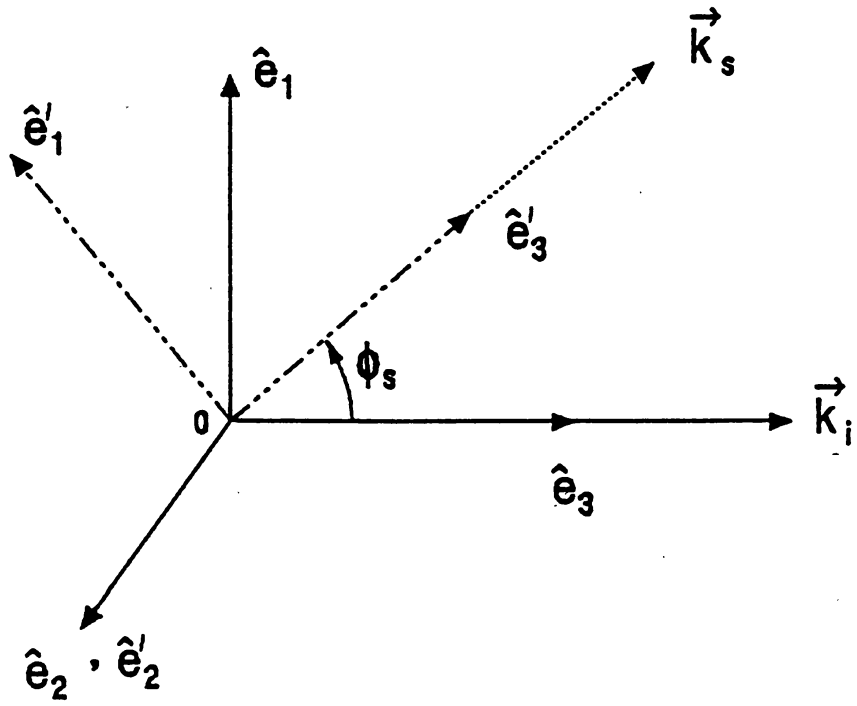

Figure 3. The wave vectors and the electric fields of the incident and the scattered radiation.

Fig. 3 shows the directions of $\vec{k_i}$ and $\vec{k_s}$ in the orthogonal coordinate systems ($\hat{e}_1$, $\hat{e}_2$, $\hat{e}_3$) and ($\hat{e}'_1$, $\hat{e}'_2$, $\hat{e}'_3$). The coordinate system ($\hat{e}'_1$, $\hat{e}'_2$, $\hat{e}'_3$) is rotated through an angle ϕ_s about an axis parallel to $\hat{e}_2$. Here, $\vec{k_i} \parallel \hat{e}'_3$, $\vec{k_s} \parallel \hat{e}'_3$ and $\hat{e}'_2 \parallel \hat{e}_2$. The unit vectors are related by

$$\hat{e}'_1 = \cos(\phi_s)\,\hat{e}_1 - \sin(\phi_s)\,\hat{e}_3, \quad \hat{e}'_2 = \hat{e}_2, \quad \hat{e}'_3 = \sin(\phi_s)\,\hat{e}_1 + \cos(\phi_s)\,\hat{e}_3. \tag{5}$$

The scattered wave in the coordinate system ($\hat{e}_1$, $\hat{e}_2$, $\hat{e}_3$) is given by

$$\vec{E}_s = \epsilon_s [\cos(\vec{k_s} \cdot \vec{r} - \omega_s t)\{\cos(\phi_s)\,\hat{e}_1 - \sin(\phi_s)\,\hat{e}_3\} + \alpha_s \cos(\vec{k_s} \cdot \vec{r} - \omega_s t + \delta_s)\,\hat{e}_2]. \tag{6}$$

The wave equation for the scattered electromagnetic wave is given by

$$\left(\nabla^2 - \frac{1}{c^2}\frac{\partial^2}{\partial t^2}\right)\vec{E_s} = \frac{4\pi}{c^2}\frac{\partial \vec{J}}{\partial t}, \tag{7}$$

where c is velocity of light and $\vec{J}$ is the current density. The components of the current density are $J_1 = -en_{e1}u_{e1} = -e\ (n_0 + \delta n_{e1})u_{e1}$, $J_2 = -en_{e2}u_{e2} = -e\ (n_0 + \delta n_{e2})u_{e2}$ and $J_3 = -en_0u_{e3}$, where u_{e1}, u_{e2} and u_{e3} are the components of the oscillation velocity $\vec{u_e}$ of electrons in the radiation fields $\vec{E_i}$ and $\vec{E_s}$. We obtain $\vec{u_e}$ from the equation :

$$\frac{\partial \vec{u_e}}{\partial t} = -\frac{e}{m_0}[\vec{E_i} + \vec{E_s}], \tag{8}$$

where e and m_0 are the charge and the rest mass of an electron.

In SRS, the scattered radiation consists of the stokes mode ($\vec{k_-}$, ω_-) and the anti-stokes mode ($\vec{k_+}$, ω_+) with electric fields

$$\vec{E}\pm = \epsilon_\pm[\cos(\vec{k_\pm}\cdot\vec{r} - \omega_\pm t)\ \{\cos(\phi_\pm)\,\hat{e}_1 - \sin(\phi_\pm)\,\hat{e}_3\} + \alpha_\pm \cos(\vec{k_\pm}\cdot\vec{r} - \omega_\pm t + \delta_-)\hat{e}_2]. \tag{9}$$

Now, separating the components of equation (7), we have

$$D_\pm E_{\pm 1} = -\frac{2\pi e^2}{m_0}\,\epsilon_i \delta n_1\left[\frac{\omega_-}{\omega_i}\cos(\vec{k_-}\cdot\vec{r} - \omega_- t) + \frac{\omega_+}{\omega_i}\cos(\vec{k_+}\cdot\vec{r} - \omega_+ t)\right] \tag{10}$$

and

$$D_\pm E_{\pm 2} = -\frac{2\pi e^2}{m_0}\,\alpha_i \epsilon_i \delta n_2\left[\frac{\omega_-}{\omega_i}\cos(\vec{k_-}\cdot\vec{r} - \omega_- t + \delta_i - \delta_e) + \frac{\omega_+}{\omega_i}\cos(\vec{k_+}\cdot\vec{r} - \omega_+ t + \delta_i + \delta_e)\right], \tag{11}$$

and

$$D_\pm E_{\pm 3} = 0, \tag{12}$$

where $E_{\pm 1} = \epsilon_\pm \cos(\phi_\pm)\cos(\vec{k_\pm}\cdot\vec{r} - \omega_\pm t)$, $E_{\pm 2} = \alpha_\pm \epsilon_\pm \cos(\vec{k_\pm}\cdot\vec{r} - \omega_\pm t + \delta_\pm)$, $E_{\pm 3} = -\epsilon_\pm \sin(\phi_\pm)\cos(\vec{k_\pm}\cdot\vec{r} - \omega_\pm t)$, $\omega_\pm = \omega_i \pm \omega$, $\vec{k_\pm} = \vec{k_i} \pm \vec{k}$ and $D_\pm = k_\pm^2 c^2 - \omega_\pm^2 + \omega_{pe}^2$. Here, $\omega_{pe} = (4\pi n_0 e^2 / m_0)^{1/2}$ is the plasma frequency. Equation (12) restricts the value of $\phi_\pm$ to 0 or π for $\epsilon_\pm \neq 0$ and $D_\pm \neq 0$.

Expressions $D_{\pm} = 0$ are the dispersion relations for the stokes mode ($\vec{k}_-$, ω_-) and the anti-stokes mode ($\vec{k}_+$, ω_+), when the following resonant conditions are satisfied :

$$\omega_i - \omega = \omega_-, \qquad \vec{k}_i - \vec{k} = \vec{k}_-,$$
$$\omega_i + \omega = \omega_+, \qquad \vec{k}_i + \vec{k} = \vec{k}_+. \tag{13}$$

Multiplying equation (10) on both sides by $\cos(\vec{k}_i . \vec{r} - \omega_i t)$ and neglecting the terms containing ($2\vec{k}_i$, $2\omega_i$) as being non-resonant, we get

$$D_{\pm}\epsilon_{\pm} \cos(\phi_{\pm}) = -\frac{4\pi e^2}{m_0}\epsilon_i \delta n_1. \tag{14}$$

Similarly, if we multiply equation (11) by $\cos(\vec{k}_i . \vec{r} - \omega_i t + \delta_i)$, we obtain

$$D_{\pm}\alpha_{\pm}\epsilon_{\pm} \cos[\vec{k} . \vec{r} - \omega t \pm (\delta_{\pm} - \delta_i)] = -\frac{4\pi e^2}{m_0}\alpha_i \epsilon_i \delta n_2 \cos(\vec{k} . \vec{r} - \omega t + \delta_e). \tag{15}$$

Similar to equations (13), it gives following conditions between the phases

$$\delta_{\pm} = \delta_i \pm \delta_e. \tag{16}$$

Dividing equation (15) by equation (4), we have

$$\alpha_{\pm} = \alpha_i \frac{\delta n_2}{\delta n_1} \cos(\phi_{\pm}) = \alpha_i R \cos(\phi_{\pm}), \tag{17}$$

where $R = \delta n_2 / \delta n_1$. The value of R is related to $\vec{E}_i$: δn_{e1} couples with $\vec{E}_{i1}$ and δn_{e2} couples with $\vec{E}_{i2}$. In the linear theory, it is not possible to determine R, but one expects that it may not differ too much from the value of α_i.

If we multiply equation (14) by ϵ_i and equation (15) by $\alpha_i\epsilon_i$, and subtract, we find

$$(\alpha_i\alpha_{\pm} - \cos\phi_{\pm})\epsilon_{\pm} = \frac{4\pi e^2}{m_0}\epsilon_i (1 - \alpha_i^2 R)\frac{\delta n_1}{D_{\pm}} \tag{18}$$

Now, we have to determine the electron density perturbations δn_1 and δn_2. Here, we neglect the ions response because of their larger mass compared to that of the electrons. With the inclusion of the ponderomotive force, as a driving force, the Vlasov equation for the low frequency response of electrons can then be written as

$$\frac{\partial f}{\partial t} + \vec{v} \cdot \nabla f + \frac{1}{m_0} (e\nabla\phi - \nabla\psi) \cdot \frac{\partial f}{\partial \vec{u}} = 0, \tag{19}$$

where $\phi(\vec{r}, t)$ is the potential associated with the electrostatic waves, $f(\vec{r}, \vec{v}, t)$, is the particle distributeion function and $\psi(\vec{r}, t)$ is the ponderomotive potential. Linearizing equation (19) with $f(\vec{r}, \vec{v}, t) = f_0(\vec{v}) + \delta f_{e1}(\vec{r}, \vec{v}, t) + \delta f_{e2}(\vec{r}, \vec{v}, t)$, we get

$$\frac{\partial(\delta f_{e1})}{\partial t} + \frac{\partial(\delta f_{e2})}{\partial t} + \vec{v}\partial \cdot \nabla(\delta f_{e1}) + \vec{v} \cdot \nabla(\delta f_{e2}) + \frac{1}{m_0} (e\nabla\phi - \nabla\psi) \cdot \frac{\partial f_0}{\partial \vec{v}} = 0, \tag{20}$$

where $\delta f_{e1} = \delta f_1 \cos(\vec{k} \cdot \vec{r} - \omega t)$ and $\delta f_{e2} = \delta f_2 \cos(\vec{k} \cdot \vec{r} - \omega t + \delta_e)$. The ponderomotive force of the radiation field is given by $\vec{F}_\omega = -\nabla\psi$. It depends quadratically on the ampliutde and leads to a slowly varying longitudinal field, corresponding physically to radiation pressure, which leads to slow longitudinal motions and modifies the density. The ponderomotive potential is given by :

$$\psi = \frac{e^2}{2m_0} \left\langle \left(\mathrm{Re} \left| \frac{\vec{E}_i}{i\omega_i} + \frac{\vec{E}_-}{i\omega_-} + \frac{\vec{E}_+}{i\omega_+} \right| \right)^2 \right\rangle_\omega$$

$$= \frac{e^2}{2m_0\omega_i^2} [\epsilon_i\epsilon_- \cos(\phi_-) \cos(\vec{k} \cdot \vec{r} - \omega t) + \alpha_i\alpha_-\epsilon_i\epsilon_- \cos(\vec{k} \cdot \vec{r} - \omega t + \delta_i - \delta_-) +$$

$$\epsilon_i\epsilon_+ \cos(\phi_+) \cos(\vec{k} \cdot \vec{r} - \omega t) + \alpha_i\alpha_+\epsilon_i\epsilon_+ \cos(\vec{k} \cdot \vec{r} - \omega t + \delta_+ - \delta_i)]. \tag{21}$$

The angular bracket $\langle \rangle_\omega$ represents the ω frequency component of an average over the fast time scale ($\omega_i >> \omega$).

To determine ϕ self-consistently we use Poisson equation, which gives

$$\phi = -\frac{4\pi e}{k^2} (\delta n_{e1} + \delta n_{e2}). \tag{22}$$

Now, subtituting the expressions for δf_{e1}, δf_{e2}, δn_{e1}, δn_{e2}, ϕ and ψ into equation (20), we have

$$\delta f_2 + \mu\delta f_1 + \frac{4\pi e^2}{m_0 k^2} \left[\delta n_2 + \mu\delta n_1 + \frac{k^2}{8\pi m_0\omega_i^2} \{\epsilon_i\epsilon_- \cos(\phi_-)\mu + \epsilon_i\epsilon_+ \cos(\phi_+)\mu +$$

$$\alpha_i\alpha_-\epsilon_i\epsilon_- \frac{\sin(\vec{k}\cdot\vec{r} - \omega t + \delta_i - \delta_-)}{\sin(\vec{k}\cdot\vec{r} - \omega t + \delta_e)} + \alpha_i\alpha_+ \epsilon_i\epsilon_+ \frac{\sin(\vec{k}\cdot\vec{r} - \omega t + \delta_+ - \delta_i)}{\sin(\vec{k}\cdot\vec{r} - \omega t + \delta_e)}\Bigg\}\Bigg] \times$$

$$\frac{\vec{k}\cdot\dfrac{\partial f_0}{\partial \vec{v}}}{(\omega - \vec{k}\cdot\vec{v})} = 0, \tag{23}$$

where $\mu = \sin(\vec{k}\cdot\vec{r} - \omega t) / \sin(\vec{k}\cdot\vec{r} - \omega t + \delta_e)$.

Equation (23) shows that $\delta_\pm = \delta_i \pm \delta_e$ and $\delta_e = 0$ or π. We obtain , for $\delta_e = \pi$,

$$\delta f_2 - \delta f_1 = -\frac{4\pi e^2}{m_0 k^2}\left[\delta n_2 - \delta n_1 + \frac{k^2}{8\pi m_0 \omega_i^2} A\right] \frac{\vec{k}\cdot\dfrac{\partial f_0}{\partial \vec{v}}}{(\omega - \vec{k}\cdot\vec{v})}, \tag{24}$$

where $A = (\alpha_i\alpha_- - \cos\phi_-)\epsilon_i\epsilon_- + (\alpha_i\alpha_+ - \cos\phi_+)\epsilon_i\epsilon_+$. The difference in the density perturbations $(\delta n_2 - \delta n_1)$ is given by

$$\delta n_2 - \delta n_1 = \int_{-\infty}^{\infty} n_0 (\delta f_2 - \delta f_1)\, d\vec{v} = -\left[\delta n_2 - \delta n_1 + \frac{k^2}{8\pi m_0 \omega_i^2} A\right] \chi_e, \tag{25}$$

where

$$\chi_e = \frac{\omega_{pe}^2}{k^2} \int_{-\infty}^{\infty} \frac{\vec{k}\cdot\dfrac{\partial f_0}{\partial \vec{v}}}{(\omega - \vec{k}\cdot\vec{v})} d\vec{v}, \tag{26}$$

is the electron susceptibility function (Liu and Kaw 1976; Fried and Conte 1961). Since $R = \delta n_2 / \delta n_1$, from equation (25) we have

$$\left(1 + \frac{1}{\chi_e}\right)(1 - R)\delta n_1 = \frac{k^2}{8\pi m_0 \omega_i^2} A. \tag{27}$$

Substituting equation (27) for δn_1 into equation (18), we obtain

$$\left(1 + \frac{1}{\chi_e}\right)(1 - R) = \frac{v_0^2 k^2}{2} \frac{(1 - R\alpha_i^2)}{(1 + \alpha_i^2)} \left(\frac{1}{D_-} + \frac{1}{D_+}\right), \tag{28}$$

where $v_0 = e\epsilon_i \sqrt{1 + \alpha_i^2} / m_0\omega_i$ is the quiver velocity of electrons in the field of incident electromagnetic wave. The energy density of the incident field and the luminosity L of the source are related by

$$\frac{1}{8\pi} \epsilon_i^2 (1 + \alpha_i^2) = \frac{L}{4\pi r^2 c}, \tag{29}$$

where r is the distance between source of radiation and plasma. Therefore, the quiver velocity of electrons is given by

$$v_0 = \frac{e}{m_0} \left(\frac{2L}{r^2 c}\right)^{1/2} \frac{1}{\omega_i}. \tag{30}$$

Equation (28) is the plasma dispersion relation describing the SRS of elliptically polarized electromagnetic wave. The SRS instability resonantly excites only when the frequency and wave number matching conditions (see equation 13) are satisfied. The simplest stimulated scattering process is the one involving only one high-frequency sideband, i.e., the stokes component $(\vec{k}_-, \omega_-)$. Thus, we consider a case where $D_- \approx 0$ and $D_+ \neq 0$, i.e., the anti-stokes components $(\vec{k}_+, \omega_+)$ is non-resonant. This approximation is justified as long as $\omega << (c^2 \vec{k}_i . \vec{k}/\omega_i)$; it breaks down for very small $\vec{k}$ (i.e., for long wavelength electrostatic perturbations) or if $\vec{k}$ is nearly perpendicular to $\vec{k}_i$).

The value of k is approximately $2k_i$, corresponding to backward scattering ($\phi_- = \pi$) and for forward scattering ($\phi_- = 0$) it is approximately ω_{pe} / c. Thus, the growth rate of the instability attains its maximum value for backscatter. For the case of backscattering, $D_-(\vec{k}_-, \omega_-) \approx 2\omega_i$ $(\omega - c^2 \vec{k}_i . \vec{k}/\omega_i + c^2k^2/2\omega_i) \approx 0$ for $\omega_i >> \omega$. The dispersion relation for primarily backscatter is, therefore,

$$\left(1 + \frac{1}{\chi_e}\right)(1 - R) = \frac{1}{4} \frac{v_0^2 k^2}{\omega_i (\omega - \Delta)} \frac{(1 - R\alpha_i^2)}{(1 + \alpha_i^2)} \tag{31}$$

where

$$\Delta = \vec{k} . \vec{v}_g - \frac{k^2 c^2}{2\omega_i} \tag{32}$$

with $\vec{v}_g = \vec{k}_i c^2 / \omega_i$. From the equation (31), we can derive the threshold and the growth rate for the SRS instability. For $\omega^2 \approx \omega_e^2 = \omega_{pe}^2 + (3/2)k^2 v_T^2$, the natural frequency of the plasma wave and $\omega_-^2 \approx \omega_{pe}^2 + c^2 (\vec{k}_i - \vec{k})^2$, equation (31) can be written as

$$(\omega - \omega_e + i\Gamma_e)\,(\omega - \omega_e + i\Gamma_-)\,(1 - R) = -\frac{v_0^2\,k^2\,\omega_{pe}}{8\omega_i}\,\frac{(1 - R\alpha_i^2)}{(1 + \alpha_i^2)}, \tag{33}$$

where

$$\Gamma_e = \frac{\sqrt{\pi}}{2}\,\frac{\omega_{pe}}{(k\lambda_{De})^3}\,\exp\left[-\frac{1}{2(k\lambda_{De})^2} - \frac{3}{2}\right] + \nu_e \tag{34}$$

is the damping rate of the electron plasma wave, $\nu_e = 3.632 n_e \ln \Lambda / T_e^{3/2}$ is the electron collision frequency and Coulomb logarithm $\ln \Lambda \approx 10$. Here $\Gamma_- = \omega_{pe}^2 \nu_e / 2\omega_-^2$ is the collisional damping rate of the scattered electromagnetic wave. Setting $\omega = \omega_e + i\Gamma$, and solving equation (33) for the growth rate Γ, we find

$$\Gamma = -\frac{1}{2}(\Gamma_e + \Gamma_-) \pm \frac{1}{2}\sqrt{(\Gamma_e - \Gamma_-)^2 + \frac{v_0^2\,k^2\,\omega_{pe}}{2\omega_i\,(1 + \alpha_i^2)}\,\frac{(1 - R\alpha_i^2)}{(1 - R)}}. \tag{35}$$

Setting $\Gamma = 0$, we obtain the threshold condition for the excitation of SRS;

$$\left(\frac{v_0}{c}\right)_{thr} = 2\,\frac{\Gamma_e\Gamma_-}{\omega_i\omega_{pe}}\,\frac{(1 + \alpha_i^2)\,(1 - R)}{(1 - R\alpha_i^2)}. \tag{36}$$

The growth rate just above the threshold is given by

$$\Gamma = \frac{v_0^2\,k^2\,\omega_{pe}}{8\,(\omega_i - \omega_{pe})\,\Gamma_e}\,\frac{(1 - R\alpha_i^2)}{(1 + \alpha_i^2)\,(1 - R)}, \tag{37}$$

which is proportional to E_i^2. The maximum growth rate attainable for $\omega_{pe} > \Gamma > \Gamma_e$, on the other hand, is

$$\Gamma = \frac{v_0 k}{2}\sqrt{\frac{\omega_{pe}}{2(\omega_i - \omega_{pe})}\,\frac{(1 - R\alpha_i^2)}{(1 + \alpha_i^2)\,(1 - R)}}. \tag{38}$$

For $k \approx 2k_i$, equation (38) becomes

$$\Gamma = \frac{e\epsilon_i}{m_0 c}\sqrt{\frac{\omega_{pe}}{2\omega_i}\,\frac{(1 - R\alpha_i^2)}{(1 - R)}}. \tag{39}$$

We note that backscatter by plasma wave is possible only if $2k_i\lambda_{De} << 1$. For $k_i\lambda_{De}$ not too small, the stimulated Compton backward scattering due to the non-linear Landau damping of the beat mode by resonant electrons becomes important.

2.1 Stokes parameters

The polarization state of the incident radiation changes due to the SRS in a plasma (see equations 1, 9, 16 with $\delta_e = 0$ or π). The stokes parameters for the incident and scattered electromagentic waves (Rybicki & Lightman 1979) are :

$$I_j = \frac{c}{8\pi}(1 + \alpha_j^2)\varepsilon_i^2 = \frac{c}{8\pi}\varepsilon_j^2 \ , \tag{40}$$

$$Q_j = \frac{(1 - \alpha_j^2)}{(1 + \alpha_j^2)} I_j, \tag{41}$$

$$U_j = \frac{2\alpha_j}{(1 + \alpha_j^2)} I_j \cos(\delta_j), \tag{42}$$

and

$$Vj = - \f(2\alpha_j(1 + \alpha\o(^2,_j))) I_j \sin(\delta_j). \tag{43}$$

The sense of rotation of the electric field is given by

$$\sin(2\beta_j) = \frac{V_j}{I_j} = -\frac{2\alpha_j}{(1 + \alpha_j^2)} \sin(\delta_j). \tag{44}$$

The magnitudes of the principle axes of the ellipse are

$$a_j = I_j \, |\cos(\beta_j)| \text{ and } b_j = I_j \, |\sin(|\beta_j)|. \tag{45}$$

The orientation of the major axis of the ellipse relative to $\hat{e}_1$ axis, is given by

$$\tan(2\chi_j) = \frac{U_j}{Q_j} = \frac{2\alpha_j}{(1 + \alpha_j^2)} I_j \cos(\delta_j). \tag{46}$$

Here, j = i for incident and – for scattered electromagnetic waves.

We use the relations $\delta_e = \pi$, $\delta_- = \delta_i - \delta_e$ and $\alpha_- = \alpha_i R$ to compute the stokes parameters for the scattered wave.

2.2 Numerical solution of equation (28)

For a strongly damped electron plasma wave with $k_l\lambda_{De} \approx 0.4$, it is not possible to expand $\chi_e(\omega, k)$ into an asymptotic series. The regime $k_l\lambda_{De} \approx 0.4$ corresponds to the transition region between SRS and stimulated Compton scattering (SCS) (Gangadhara & Krishan 1992). Therefore, using $\omega = \omega_e + i\Gamma$, we numerically solve equation (28) including all the damping effects.

2.2.1 In pulsars

The typical values of the plasma and radiation parameters at a distance r = $100R_{NS} = 10^8$ cm, (Neutron star radius RNS ≈ 10 km), in a pulsar are electron density $n_e = n_8 \times 10^8$ cm^{-3}, temperature $T_e = T_5 \times 10^5$ K and luminosity $L = L_{30} \times 10^{30}$ erg / sec in the band $\Delta\nu < \nu =$ 600 MHz (Gangadhara *et al.* 1992).

Fig. 4 shows the e-folding time $t_e = 1/\Gamma$ as a function of ω_i / ω_{pe} at the different values of electron temperature T_e (= 10^5, 5 x 10^5, 10^6, and 7.5 x 10^6 K) for forward SRS of the incident wave. The frequency of the scattered electromagnetic wave is $\omega_- = \omega_i + \omega_e$. One recalls that at high temperatures an electron plasma wave experiences a small collisional damping but large Landau damping. The rather fast rise in t_e is obtained in the SCS regime ($k_e\lambda_{De} \geq 0.4$). The points indicated by C correspond to $k_e\lambda_{De} \approx 0.4$ and represent the change of scattering process from Raman to Compton.

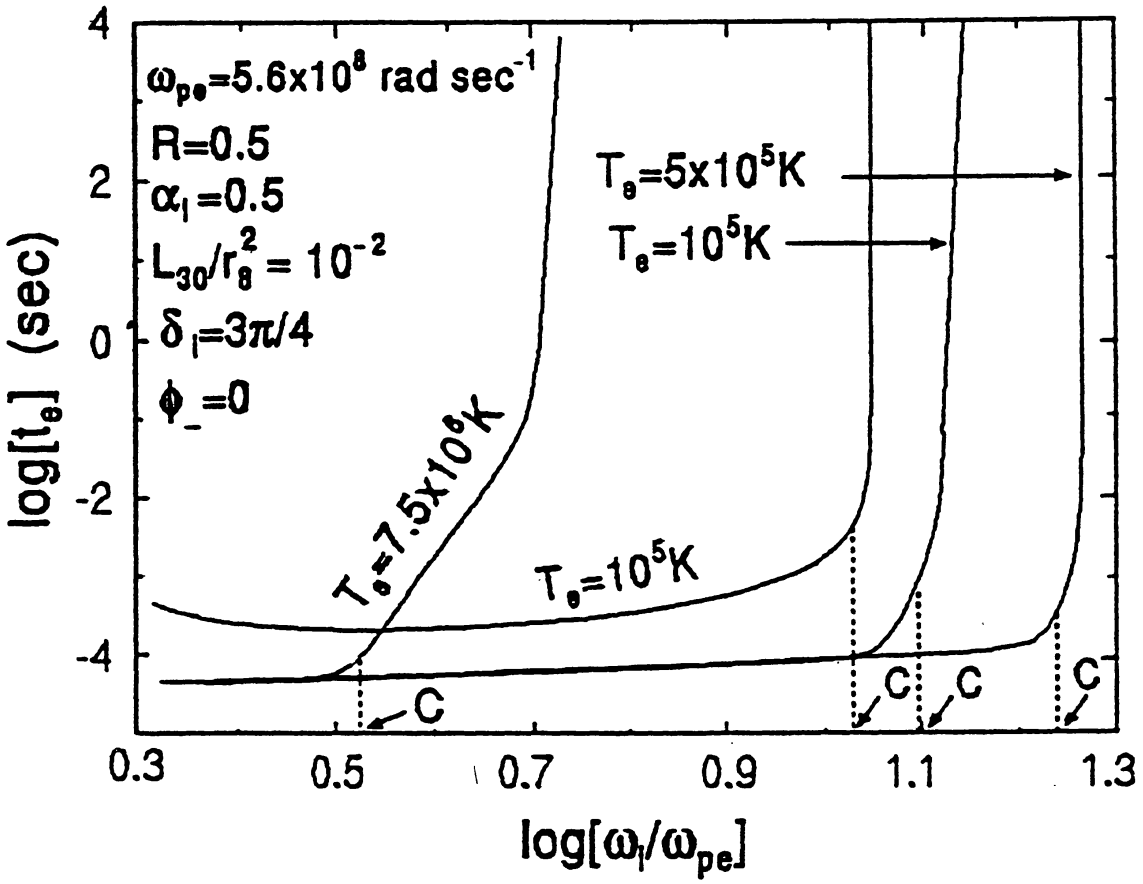

Figure 4. The e-folding time $t_e = 1/\Gamma$ versus the normalized frequency (ω_i / ω_{pe}). The points C represent the transition between SRS and SCS, where $k_i\lambda_{De} \approx 0.4$. At lower values of ($\omega_i / \omega_{pe}$) SRS occurs while at higher values SCS occurs.

We know from the observations of pulsar PSR B1133 + 16 by Cordes (1983) that flux $I_i = 10^{-20}$ erg cm^{-2} Hz^{-1} at the radio frequency $\nu_i = 600$ MHz. To find the relation between the incident flux I_i and the scattered flux I_- we use condition for conservation of wave-energy within the system of waves, the Manley-Rowe relation (Weiland & Wilhelmsson 1977), given by

$$\frac{I_i}{\omega_i} = \frac{I_-}{\omega_-} . \tag{47}$$

It gives

$$I_- = \left(1 - \frac{\omega}{\omega_i}\right) I_i . \tag{48}$$

For $\omega \approx \omega_{pe}$ and $\omega_i = 2.5\ \omega_{pe}$, we get $I_- = 0.6\ I_i$. The sense of rotation and the orientation of the ellipses of the incident and the forward scattered electromagnetic waves are shown in Fig. 5.

In Table 1, the values of stokes parameters for the incident and the forward scattered electromagnetic waves in the pulsar PSR B1133 + 16 are listed. It shows that : (1) a linearly polarized incident elecromagnetic wave ($\delta_i = \pi$, $\alpha_i = 0.5$) scatters into another linearly polarized electromagnetic wave with its plane of polarization rotated through an angle χ_- with respect to $\hat{e}_l$ axis (see Fig. 5); (2) a elliptically polarized incident wave with counterclockwise sense ($\delta_i = 3\pi/4$, $\alpha_i = 1$) scatters into (i) a linearly polarized wave when R = 0, (ii) elliptically polarized waves with clockwise sense with major axis rotated thorough an angle χ_- when R = 0.4, 0.8 & 1.2; (3) a circlularly polarized incident wave with counterclockwise sense ($\delta_i = \pi/2$, $\alpha_i = 1$) scatters into (i) linearly polarized wave when R = 0, (ii) an elliptically polarized wave with clockwise sense when R = 0.4 & 0.8, (iii) a circularly polarized wave with clockwise sense when R = 1.

Similar to the Table 1, the stokes parameters of the incident and backward scattered electromagnetic waves in PSR B1133 + 16 are listed in Table 2. In the case of backward SRS sense reversal does not occur.

Fig. 6 shows χ_- as a function of the e-folding time t_e, for different values of α_i in the case of forward scattering of the elliptically polarized radio wave $\vec{E}_i$, in the emission region of a pulsar. Here, R is varied between 0 and 1. For R close to 1, one observes $t_e \leq 10^4$ sec. The rotational angle χ_- reaches a maximum when the growth rate attains its maximum. It is seen that a reversal in the sense of polarization can take place in a time scale lying between micro to milliseconds.

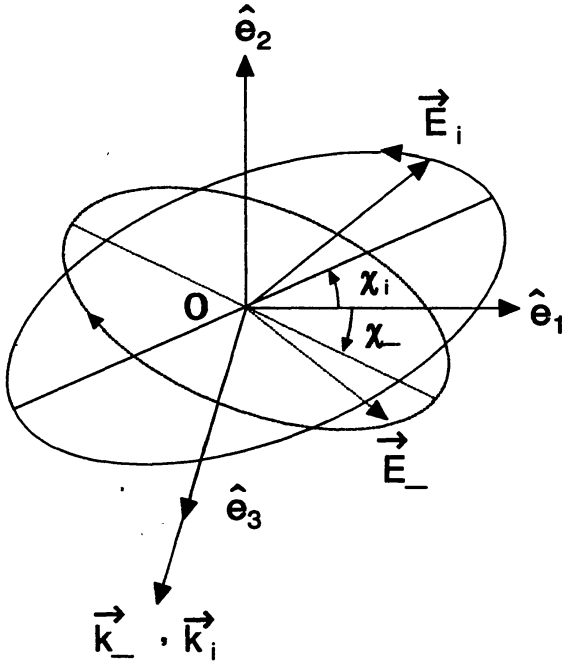

Figure 5. The ellipses of the electric fields of the incident and forward scattered electromagnetic waves.

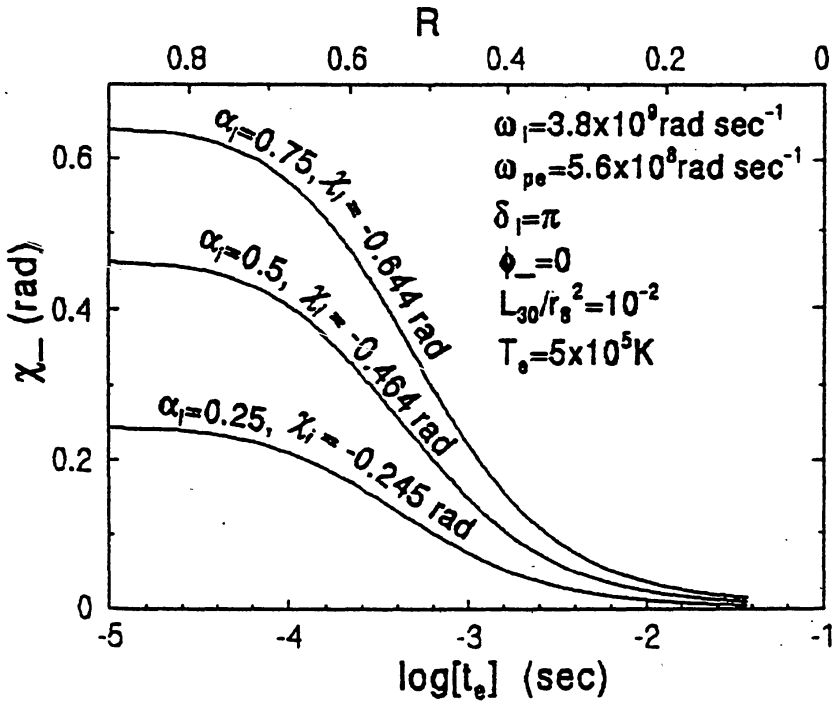

Figure 6. The orientation angle χ_- of the scattered radiation versus the e-folding time t_e for the SRS scttering of radio waves in a pulsar.

Table 1

Stokes parameters of the incident and forward scattered EM waves for PSR 1133+16

Parameters (erg cm^{-2}sec^{-1}Hz^{-1})	Incident wave $\delta_i = \pi$, $\alpha_i = 0.5$	Scattered wave $\delta_- = 0$			
		R=0	R=0.4	R=0.8	R=1.2
I	1.0000E-20	6.0000E-21	6.0000E-21	6.0000E-21	6.0000E-21
Q	6.0000E-21	6.0000E-21	5.5385E-21	4.3448E-21	2.8235E-21
U	-8.0000E-21	0.0	2.3077E-21	4.1379E-21	5.2941E-21
V	0.0	0.0	0.0	0.0	0.0
χ (rad)	-0.4636	0.0	0.1974	0.3805	0.5404
a	1.0000E-20	6.0000E-21	6.0000E-21	6.0000E-21	6.0000E-21
b	0.0	0.0	0.0	0.0	0.0
Sense of rotation	...	...	...	...	...
Nature	linear	linear	linear	linear	linear

Parameters (erg cm^{-2}sec^{-1}Hz^{-1})	Incident wave $\delta_i = 3\pi/4$, $\alpha_i = 1$	Scattered wave $\delta_- = -\pi/4$			
		R=0	R=0.4	R=0.8	R=1.2
I	1.0000E-20	6.0000E-21	6.0000E-21	6.0000E-21	6.0000E-21
Q	0.0	6.0000E-21	4.3448E-21	1.3171E-21	-1.0820E-21
U	-7.0711E-21	0.0	2.9260E-21	4.1392E-21	4.1731E-21
V	-7.0711E-21	0.0	2.9260E-21	4.1392E-21	4.1731E-21
χ (rad)	...	0.0	0.2963	0.6314	-0.6586
a	9.239E-21	6.0000E-21	5.8064E-21	5.5705E-21	5.5618E-21
b	3.8268E-21	0.0	1.5118E-21	2.2291E-21	2.2510E-21
Sense of rotation	counter–clockwise	...	clockwise	clockwise	clockwise
Nature	elliptical	linear	elliptical	elliptical	elliptical

Parameters (erg cm^{-2}sec^{-1}Hz^{-1})	Incident wave $\delta_i = \pi/2$, $\alpha_i = 1$	Scattered wave $\delta_- = -\pi/2$			
		R=0	R=0.4	R=0.8	R=1
I	1.0000E-20	6.0000E-21	6.0000E-21	6.0000E-21	6.0000E-21
Q	0.0	6.0000E-21	4.3448E-21	1.3171E-21	0.0
U	0.0	0.0	0.0	0.0	0.0
V	-1.0000E-20	0.0	4.1379E-21	5.8536E-21	6.0000E-21
χ (rad)	...	0.0	2.9170E-17	1.3613E-16	...
a	7.0711E-21	6.0000E-21	5.5709E-21	4.6852E-21	4.2426E-21
b	7.0711E-21	0.0	2.2283E-21	3.7482E-21	4.2426E-21
Sense of rotation	counter–clockwise	...	clockwise	clockwise	clockwise
Nature	circular	linear	elliptical	elliptical	circular

Table 2

Stokes parameters of the incident and backward scattered EM waves for PSR 1133+16

Parameters ($erg\ cm^{-2}sec^{-1}Hz^{-1}$)	Incident wave $\delta_i = \pi$, $\alpha_i = 0.5$	Scattered wave $\delta_- = 0$			
		R=0	R=0.4	R=0.8	R=1.2
I	1.0000E-20	6.0000E-21	6.0000E-21	6.0000E-21	6.0000E-21
Q	6.0000E-21	6.0000E-21	5.5385E-21	4.3448E-21	2.8235E-21
U	-8.0000E-21	0.0	-2.3077E-21	-4.1379E-21	-5.2941E-21
V	0.0	0.0	0.0	0.0	0.0
χ (rad)	-0.4636	0.0	-0.1974	-0.38051	-0.54042
a	1.0000E-20	6.0000E-21	6.0000E-21	6.0000E-21	6.0000E-21
b	0.0	0.0	0.0	0.0	0.0
Sense of rotation	...	...	...	...	...
Nature	linear	linear	linear	linear	linear

Parameters ($erg\ cm^{-2}sec^{-1}Hz^{-1}$)	Incident wave $\delta_i = 3\pi/4$, $\alpha_i = 1$	Scattered wave $\delta_- = -\pi/4$			
		R=0	R=0.4	R=0.8	R=1.2
I	1.0000E-20	6.0000E-21	6.0000E-21	6.0000E-21	6.0000E-21
Q	0.0	6.0000E-21	4.3448E-21	1.3171E-21	-1.0820E-21
U	-7.0711E-21	0.0	-2.9260E-21	-4.1392E-21	-4.1731E-21
V	-7.0711E-21	0.0	-2.9260E-21	-4.1392E-21	-4.1731E-21
χ (rad)	-0.7854	0.0	-0.2963	-0.6314	0.6586
a	9.2388E-21	6.0000E-21	5.8064E-21	5.5705E-21	5.5618E-21
b	3.8268E-21	0.0	1.5118E-21	2.2291E-21	2.2510E-21
Sense of rotation	counter-clockwise	...	counter-clockwise	counter-clockwise	counter-clockwise
Nature	elliptical	linear	elliptical	elliptical	elliptical

Parameters ($erg\ cm^{-2}sec^{-1}Hz^{-1}$)	Incident wave $\delta_i = \pi/2$, $\alpha_i = 1$	Scattered wave $\delta_- = -\pi/2$			
		R=0	R=0.4	R=0.8	R=1
I	1.0000E-20	6.0000E-21	6.0000E-21	6.0000E-21	6.0000E-21
Q	0.0	6.0000E-21	4.3448E-21	1.3171E-21	0.0
U	0.0	0	0.0	0.0	0.0
V	-1.0000E-20	0.0	-4.1379E-21	-5.8537E-21	-6.0000E-21
χ (rad)	...	0.0	-2.9170E-17	-1.3612E-16	...
a	7.0711E-21	6.0000E-21	5.5709E-21	4.6852E-21	4.2426E-21
b	7.0711E-21	0.0	2.2283E-21	3.7482E-21	4.2426E-21
Sense of rotation	counter-clockwise	...	counter-clockwise	counter-clockwise	counter-clockwise
Nature	circular	linear	elliptical	elliptical	circular

Table 3

Stokes parameters of the incident and forward scattered EM waves for 3C 273

Parameters (erg $cm^{-2}sec^{-1}Hz^{-1}$)	Incident wave $\delta_i = \pi$, $\alpha_i = 0.5$	Scattered wave $\delta_- = 0$			
		R=0	R=0.4	R=0.8	R=1.2
I	4.2266E-22	2.5360E-22	2.5360E-22	2.5360E-22	2.5360E-22
Q	2.5360E-22	2.5360E-22	2.3410E-22	1.8364E-22	1.1934E-22
U	-3.3813E-22	0.0	9.7537E-23	1.7490E-22	2.2376E-22
V	0.0	0.0	0.0	0.0	0.0
χ (rad)	-0.4636	0.0	0.1974	0.3805	0.5404
a	4.2266E-22	2.5360E-22	2.5360E-22	2.5360E-22	2.5360E-22
b	0.0	0.0	0.0	0.0	0.0
Sense of rotation	...	...	...	...	...
Nature	linear	linear	linear	linear	linear

Parameters (erg $cm^{-2}sec^{-1}Hz^{-1}$)	Incident wave $\delta_i = 3\pi/4$, $\alpha_i = 1$	Scattered wave $\delta_- = -\pi/4$			
		R=0	R=0.4	R=0.8	R=1.2
I	4.2266E-22	2.5360E-22	2.5360E-22	2.5360E-22	2.5360E-22
Q	0.0	2.5360E-22	1.8364E-22	5.5667E-23	-4.5730E-23
U	-2.9887E-22	0.0	1.2367E-22	1.7495E-22	1.7640E-22
V	-2.9887E-22	0.0	1.2367E-22	1.7495E-22	1.7638E-22
χ (rad)	-0.7854	0.0	0.2963	0.6314	-0.6586
a	3.9049E-22	2.5360E-22	2.4541E-22	2.3544E-22	2.3507E-22
b	1.6174E-22	0.0	6.3896E-23	9.4217E-23	9.5139E-23
Sense of rotation	counter-clockwise	...	clockwise	clockwise	clockwise
Nature	elliptical	linear	elliptical	elliptical	elliptical

Parameters (erg $cm^{-2}sec^{-1}Hz^{-1}$)	Incident wave $\delta_i = \pi/2$, $\alpha_i = 1$	Scattered wave $\delta_- = -\pi/2$			
		R=0	R=0.4	R=0.8	R=1
I	4.2266E-22	2.5360E-22	2.5360E-22	2.5360E-22	2.5360E-22
Q	0.0	2.5359E-22	1.8364E-22	5.5667E-23	0.0
U	0.0	0.0	0.0	0.0	0.0
V	-4.2266E-22	0.0	1.7489E-22	2.47410E-22	2.5360E-22
χ (rad)	....	0.0	2.9170E-17	1.3612E-16	...
a	2.9886E-22	2.5359E-22	2.3545E-22	1.9802E-22	1.7932E-22
b	2.9886E-22	0.0	9.4183E-23	1.5842E-22	1.7932E-22
Sense of rotation	counter-clockwise	...	clockwise	clockwise	clockwise
Nature	circular	linear	elliptical	elliptical	circular

2.2.2 In quasars

The typical values of the plasma and radiation parameters in the broad-line region, at a distance $r = r_{pc} \times 3.086 \times 10^{18}$ cm from the central engine of a quasar are (Krishan & Wiita 1990; Gangadhara & Krishan 1990) electron density $n_e = n_9 \times 10^9$ cm^{-3}, temperature $T_e = T_5 \times 10^5$ K and luminosity $L = L_{42} \times 10^{42}$ erg / sec in the radio band $\Delta\omega \approx \omega_{pe}$.

Fig. 7 shows χ_- as a function of the e-folding time t_e, for different values of α_i for forward scattering of the elliptically polarized radio wave $\vec{E}_i$ in a quasar. The rotational angle χ_- reaches a maximum when the growth rate attains its maximum. Similarly, Fig. 8 shows χ_- as a function of the e-folding time t_e, at different values of α_i for forward scattering of the elliptically polarized optical wave $\vec{E}_i$ in a quasar.

We know from the multifrequency observations of 3C 273 by Courvoisier *et al.* (1987) that $I_i = 4.2266 \times 10^{-22}$ erg cm^{-2} sec^{-1} Hz^{-1} at the radio frequency $\nu_i = 6.366 \times 10^9$ Hz. For $\omega \approx \omega_{pe}$ and $\omega_i = 2.5\ \omega_{pe}$, we obtain from equation (48) that $I_- = 2.5360 \times 10^{-22}$ erg cm^{-2} sec^{-1} Hz^{-1}.

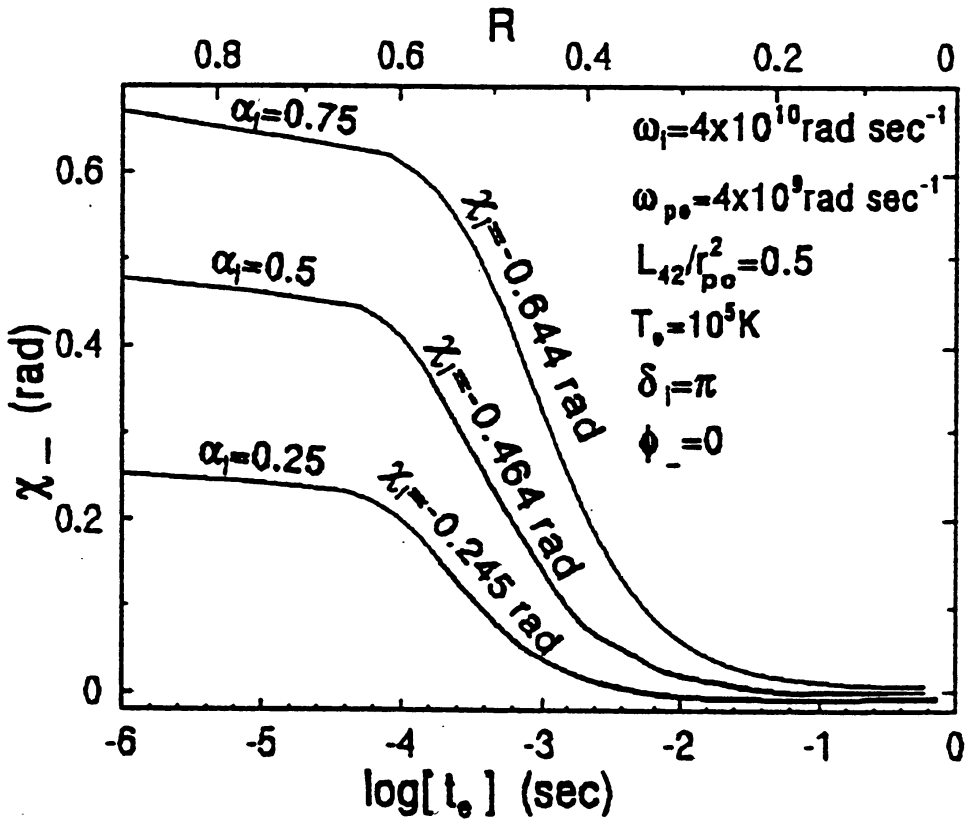

Figure 7. The orientation angle χ_- of the scattered radiation versus the e-folding time t_e for the SRS scttering of radio waves in a quasar.

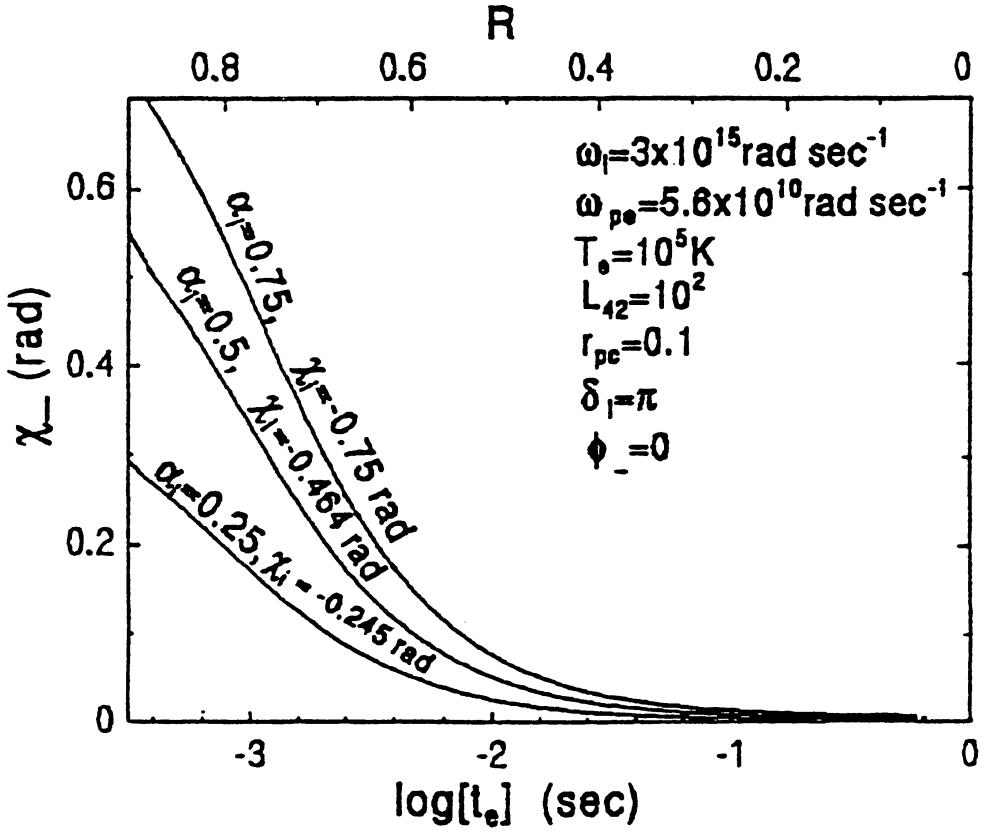

Figure 8. The orientation angle χ_- of the scattered radiation versus the e-folding time t_e for the SRS scattering of optical waves in a quasar.

Similar to Table 1, in Table 3 the values of stokes parameters for the incident and the forward scattered electromagnetic waves in a quasar 3C 273 are listed. It has been observed that the variability in polarization of non-thermal radiation varies over the time scales between a second to a day.

2.3 Faraday rotation versus SRS

Here, we make a comparison between the rotations of the plane of polarization produced by Faraday rotation and forward SRS, using the typical plasma and radiation parameters for a quasar. A linearly polarized electromagnetic wave which is incident on a plama, will be Faraday rotated through ΩF rad, where ΩF is given by (Lang 1974)

$$\Omega F = \frac{2.36 \times 10^4}{\nu^2} \int_0^L n_e H \cos(\theta)\, dl \text{ rad}, \tag{49}$$

after traversing a thickness, L, of the plasma. Here, H is the magnetic field and θ is the angle between the line of sight and the direction of the magnetic field. For $n_e = n_9 \times 10^9$ cm^{-3}, $H = H_{-3} \times 10^{-3}$ G and $\nu = \nu_9 \times 10^9$ Hz in the broad-line region of quasar, we get

$$\Omega_F = 2.36 \times 10^{-8} \frac{n_9 H_{-3} L}{\nu_9^2} \text{ rad.} \tag{50}$$

Consider the point log $[t_e] = -5$ sec and $\chi_- = 0.65$ rad in Fig. 7 on the curve with $\alpha_i = 0.75$ and $\chi_i = -0.644$ rad. The angle through which the plane of polarization rotated due to SRS is given by $\Omega_{SRS} = \chi_- - \chi_i = 1.294$ rad during the time $t_e = 10^{-5}$ sec. To compare Ω_F and Ω_{SRS} we need to convert t_e into the light travel distance $l = ct_e = 3 \times 10^5$ cm. Now, for $n_9 = 5$, $H_{-3} = 1$, and $\nu_9 = 6.366$ (Fig. 7) we get $\Omega_F = 8.735 \times 10^{-4}$ rad, much smaller than Ω_{SRS}.

2.4 Large amplitude electromagnetic waves and the effect of their incoherence on SRS instability

We derived the above results assuming the incident field to be monochromatic. In reality, however, some amount of incoherence is always present. It has been shown by Tamour (1973) and Thomson *et al.* (1974) that the effect of finite bandwidth $\Delta\omega_i$ of the incident field on the instability can be taken care of by replacing the damping rate of the sidebands Γ_L by $(\Gamma_L + 2\xi) \approx (\Gamma_L + \Delta\omega_i)$ where ξ is the number of phase jumps per unit time. This happens because Γ_L is a measure of the duration of time an electron is allowed to oscillate with the driving field before being knocked out of phase by a collision. The same effect results when the driving field suffers a phase shift and the two effects are additive. Thus replacing Γ_L by $\Gamma_L + \Delta\omega_i$ centainly raises the threshold for the instability.

If Γ is the growth rate due to a monochromatic pump at ω_i, then the actual growth rate Γ' due to the broad pump with a spectral width $\Delta\omega_i >> \Gamma$ is given by (Kruer 1988)

$$\Gamma' = \frac{1}{\Delta\omega_i} \Gamma^2. \tag{51}$$

Thus, the reduction in the growth rate due to the finite bandwidth may be compensated to some extent by the large luminosity radiation believed to be generated by coherent emission processes. Hence, the presence of incoherence through finite band width in the radiation field effectively increases the damping rates and the thresholds, and therefore reduces the growth rate (t_e increases) of SRS instability.

Several coherent processes like (i) emission from bunches of relativistic electron beams (Ruderman & Sutherland 1975, (ii) Curvature radiation (Gil & Snakowski 1990a, 1990b; Asséo, *et al.* 1980) and (iii) parallel acceleration mechanism (Melrose 1978) have been proposed for the radio emission from pulsars. On the other hand, the role of the coherent emission processes for the generation of continuum emission of the quasar was emphasized long back (Burbidge & Burbidge 1967) and has now begun to receive the attention it deserves

(Lesch & Pohl 1992; Krishan & Wiita 1990; Weatherall & Benford 1991; Baker *et al.* 1988; Gangadhara & Krishan 1992).

Baker *et al.* (1988) constructed a model of the inner portions of astrophysical jets, in which a relativistic electron beam is injected from the central engine into the jet plasma. This beam drives electrostatic plasma wave turbulence, which lead to the collective emission of electromagnetic waves. Weatherall and Benford (1991) describe the scattering of charged particles from an intense localized electrostatic fields (cavitons) associated with plasma turbulence. These cavitons arise from a process know as plasma collapse (Zakharov 1972), in which electrostatic energy accumulates in localized wave packets. When the beam is ultra-relativistic, the emitted radiation is enhanced by relativistic beaming along the direction of propagation. In the same spirit, in this paper, we have studied the scattering of coherent electromagnetic radiation by electron density fluctuations or Langmuir waves of different phases in order to explain the polarization changes.

Analysis of the data by University of Michigan (Aller *et al.* 1991) in the cm-wavelength regime showed both flux and linear polarization variability, and in addition polarization frequently exhibited position angle swings and large changes in percentage of polarization. To explain these observational results one incorporates shock models with special geometries. While SRS, without invoking many constraints, can explain these results.

Sillanpää, *et al.* (1991) observed rotation of polarization position angle linearly 55° in five hours, in all five colours, in the optical regime. This is the fastest ever observed position angle swing at optical regions in OJ 287 or blazar. It is difficult to explain this observed position angle swing with shocks in jet model.

3. Summary

We have explained the results of analytical as well as numerical investigations of radiation-plasma interaction instabilities in astrophysical plasmas. We investigated the role of collective plasma phenomena in the (1) generation of non-thermal power-law spectrum of quasars, (2) radio frequency heating, (3) polarization variability and (4) rapid flux variability in BL Lacs and quasars and the production of micropulses in pulsars.

The non-thermal continuum of quasars is believed to be produced through the combined action of synchrotron and inverse Compton processes, which are essentially single-particle processes. Collective plasma processes can *duplicate* all features of ordinary single-particle synchrotron emission, while greatly enhancing the emissivity (Gangadhara and Krishan 1992). Astrophysicists have long been assumed synchrotron emission as the *default* choice, since no one could make a case for other, more powerful mechanisms.

Collective plasma processes such as SRS and SCS of electromagnetic waves from relativistic electron beams, can amplify both the frequency as well as the flux. We find SRS is much faster than SCS and hence relativistic electron beam decelerates much faster due to SRS.

The power-law spectrum of the quasar 3C 273 can be reproduced from a relativistic electron beam (Gangadhara and Krishan 1992).

Radiation with frequency close to the plasma frequency can be anomalously absorbed in a plasma, due to parametric decay instability (PDI) (Gangadhara and Krishan 1990). This instability causes anomalous absorption of intense electromagnetic radiation under specific conditions of energy and momentum conservation and thus cause anomalous heating of the plasma. The rise in plasma temperature is determined by luminosity of the radio radiation and plasma parameters. It is believed that this process may be taking place in many astrophysical objects. For example, the conditions in the sources 3C 273, 3C 48 and Crab Nebula are shown to be conducive to the excitation of parametric decay instability (Gangadhara and Krishan 1990). This process can also contribute towards the absorption of 21 cm radiation, which is otherwise mostly attributed to neutral hydrogen regions (Krishan 1988). With this phenomenon one can explain the strong radio frequency heating in BL Lacs and quasars. Decay instability may be the mechanism for the formation of hot lower density corona adjoining each photoionized dense region. The dip in the spectrum of 3C 273 at 5.0×10^9 Hz (Cowsik and Lee, 1982; Wiita 1985) may be due to the anomalous absorption of radio waves through PDI. Since the growth rate of parametric decay instability is much higher than collisional damping rate of electromagnetic wave, this dip cannot be due to collisional damping alone. Compared to all other heating processes reviewed by Davidson and Netzer (1979), PDI is a faster process. Since PDI is fast and efficient process, it must be included while accounting for the observed value of the radio luminosity which is less than that obtained by extrapolation from the high frequency part of the spectrum.

Usually, when one talks about polarization change, one is referring to the same wave. SRS however brings about change of frequency but when the frequency of the incident wave is much higher than the plasma frequency, the scattered wave frequency differs very little from the incident wave frequency. Similar to the frequency and wave number matching conditions (see eqn. 13) we found conditions between the phases δ_i, $\delta_\pm$ and δ_e (see eqn. 16) in the process of three-wave interaction. Through SRS the clockwise polarized radiation can change into counterclockwise polarized radiation and vice versa. In addition, circularly polarized wave can change into a linearly polarized, a circularly polarized or an elliptically polarized wave or vice versa. The SRS also mimics Faraday rotation but at a tremendously enhanced rate.

A direct measurement of the growth rate cannot be done by a remote observer. The e-folding time represents a characteristic time during which a significant change in the degree of polarization, sense and rotation of plane of polarization takes place. Therefore, the observed variability time should be of the order of or few times the e-folding time.

The features like a large change in rotation of polarization plane, sense reversal and extremely rapid temporal changes would help to explain many observations, for which, the existing mechanisms prove to be inadequate. Because of the very strong dependence of rotation angle on plasma parameters via the growth rate, in an inhomogeneous plasma medium the depolarization, sense and rotation of plane of polarisation is a natural outcome. We believe

that the plasma process such as the SRS may be a potential mechanism for the polarization variability in pulsars and quasars.

We have investigated the modulational instability of an EM wave with electrostatic density fluctuations in an electron-positron plasma including the relativistic mass variation. Tajima and Tanuiti (1990) investigated the non-linear interaction of EM wave and acoustic modes in an electron-positron plasma, invoking the assumption of quasi-neutrality in the dynamics of plasma slow motion and ignoring relativistic mass variations of charged particles. The ponderomotive force of the EM wave leads to the excitation of low-frequency density perturbations. The modulational instability of an EM wave produces localized EM pulses. This is an intrinsic process since it occurs in the source itself. The electron-positron plasma is modulationally unstable for either linear or circular polarization. We believe that a plasma process such as modulational instability is a potential mechanism for the rapid variability and the production of micropulses in AGN and pulsars.

A strong magnetic field can also affect the collective processes. So it has to be taken into account in future work with more realistic plasma and radiation parameters. Collective plasma processes must be included in the scheme of understanding astrophysical plasmas.

The details of this article can be found in the Ph. D. thesis by Gangadhara (1993).

Acknowledgements

I am thankful to Prof. Vinod Krishan and many others for the guidance and suggestions during the course of this work.

References

Aller M.F., Aller H.D., Hughes P.A., 1991, in Extragalactic Radio Sources – From Beams to Jets, 7th IAP Meeting, ed. Roland J., Sol H. & Pelletier G., Cambridge Univ. Press, p. 167.

Asséo E., Pellat R., Sol H., 1980, Pulsars, IAU Symp. No 95, eds. Sieber W. & Wielebinski R., Reidel, Dordrecht, p. 111.

Baker D.N., Borovsky J.E., Benford G., Eilek J.A., 1988, ApJ., 326, 110.

Burbidge G.R., Burbidge E.M., 1967, Quasi-Stellar-Objects, Freeman, San Francisco.

Cordes J.M., 1983, in Proc. Conference No. 101, on Positron – Electron pairs in Astrophysics, eds. M.L. Burns, A.K. Harding & R. Ramaty, American Institute of Physics, p. 98.

Courvoisier T.J.L., *et al.* 1987, A&A, 176, 197.

Cowsik R., Lee Y.C., 1982, Proc. R. Soc. London Ser. A 383, 409.

Davidson K., Netzer H., 1979, Rev. Mod. Phys., 51, 715.

Fried D., Conte S.D., 1961, The Plasma Dispersion Function, Academic Press, New York.

Gangadhara R.T., Krishan V., 1990, J. A&A, 11, 515.

Gangadhara R.T., Krishan V., 1992, MNRAS, 256, 111.

Gangadhara R.T., Krishan V., Shukla P.K., 1993, MNRAS, 262, 151.

Gangadhara R.T., Krishan V., 1993, ApJ, 415, 505.

Gangadhara R.T., Krishan V., 1995, ApJ, 440, 116.

Gandhara R.T., 1993, Ph.D. thesis, Nonlinear propagation of intense electromagnetic waves in quasar and pulsar plasmas, Joint Astronomy Programme, Indian Institute of Science, Bangalore.

Gil J.A., Snakowski J.K., 1990 a, A&A, 234, 237.

Gil J.A., Snakowski J.K., 1990 b, A&A, 234, 269.

Heeschen D.S., Krichbanm T., Schalinski C.J., Witzel A.,1987, AJ, 94, 1493.

Krishan V., 1988, MNRAS, 231, 353.

Krishan V., Wiita, P.J. 1990, MNRAS, 246, 597.

Kruer W.L., 1988, The Physics of Laser-Plasma interactions, Addison-Wesley, New York, p. 70.

Lang K.R. 1974, Astrophysical Formulae, Springer–Verlag, p. 57.

Lesch H., Appl S., Camenzind M., 1989, A&A, 225, 341.

Lesch H., Pohl M., 1992, A&A, 254, 29.

Liu C.S., Kaw P.K., 1976, Advances in Plasma Phys., ed. Simon A. & Thompson W.B., (Interscience New York), 6, p. 83.

Lyne A.G., Graham-Smith F., 1990, Pulsar Astronomy, Cambridge Univ. Press, p 24.

Manchester N.R., Taylor H., 1977, Pulsars, W.H. Freeman, San Francisco, p. 49.

Melrose D.B., 1978, ApJ, 225, 557.

Quirrenbach A., 1990, in Meeting on Variability of Active Galactic Nuclei, eds. Miller H.R. & Wiita P.J., Cambridge Univ. Press, p. 165.

Röser H.J. Meisenheimer K., 1987, ApJ, 314, 70.

Ruderman M, Sutherland P., 1975, ApJ, 196, 51.

Rybicki G.B., Lightman A.P. 1979, Radiative Processes in Astrophysics, Wiley-Interscience, p. 62.

Sillanpää A., Nilsson K., Takalo L.O., 1991, in Extragalactic Radio Sources – From Beams to Jets, 7th IAP Meeting, ed. Roland J., Sol H. & Pelletier G., Cambridge Univ. Press, p 174.

Tajima T., Taniuti T., 1990, Phys. Rev. A, 42, 3587.

Tamour S., 1973, Phys. Fluids, 16, 1169.

Thomson J.J., Kruer W.L., Bodner S.E., DeGroot J., 1974, Phys. Fluids, 17, 849.

Weatherall J.C., Benford G., 1991, Astrophys J., 378, 543.

Weiland J., Wilhelmsson H., 1977, Coherent Non-Linear Interaction of Waves in Plasmas, Pergamon press, p. 60.

Wiita P.J., 1985, Phys. Repts. 123, 117.

Zakharov V.E., 1972, Sov. Phys. JETP, 35, 908.